DISTRIBUTED SPACECRAFT WITH HEURISTIC INTELLIGENCE TO MONITOR WILDFIRE SPREAD FOR RESPONSIVE CONTROL

Sreeja Nag[1], Vinay Ravindra[1], Richard Levinson[2], Mahta Moghaddam[3], Kurtis Nelson[4], Jan Mandel[6], Adam Kochanski[5], Angel Farguell Caus[5], Amer Melebari[3], Archana Kannan[3], Ryan Ketzner[1]

[1] Bay Area Environmental Research Institute at NASA Ames Research Center, Moffet Field, CA, [2] KBR Wyle LLC at NASA Ames Research Center, Moffet Field, CA, [3] University of Southern California, Los Angeles, CA, [4] EROS Center at United States Geological Survey, Sioux Falls, SD, [5] San Jose State University, CA & Utah State University, UT, [6] University of Colorado, Denver, CO

ABSTRACT

We develop and verify a space-based, distributed, adaptive intelligent, responsive New Observing System (NOS) to improve wildfire response decisions by monitoring and forecasting fuel flammability and wildfire spread and providing on-demand fire danger and burnt area maps. We use Global Navigation Satellite System Reflectometry (GNSS-R) as the NOS, informed by improvements to existing frameworks - D-SHIELD (Distributed Spacecraft with Heuristic Intelligence to Enable Logistical Decisions) and WRFx (Weather Research and Forecasting Fire Spread Model). Five new products are developed/enhanced using GNSS-R data from CYGNSS (7-sat NASA mission) and Spire Global (commercial fleet) and assimilated into WRFx, which improves existing USGS fire danger and LANDFIRE fuel layers products. These products are expected to inform observation planning and fire management via an observation value framework and a fire forecast reporter that we develop. Adaptive intelligence to dynamically task the observing (satellites) and planning (ground stations) assets, and synchronization between them, is achieved using novel Monte Carlo Tree Search (MCTS) based planner.

1. INTRODUCTION

GNSS-R measures L1 band signals from any GNSS network reflected off the Earth surface within the field-of-view of each satellite's receiving antenna, and geophysical properties are inferred from it. GNSS-R uses microwave data that can pierce through clouds/smoke/canopy, has a small form factor allowing for scalable constellations, and hence frequent data products during active fires than MODIS and VIIRS (12-24 hours). D-SHIELD is a software suite for optimizing ground-based, observation and data delivery planning for a constellation of spaceborne instruments, informed by dynamic scientific objectives that guarantee responsiveness to evolving phenomena [1,4]. Components of D-SHIELD have been applied to applications like imaging, floods, cyclones [22-24]. WRFx is an integrated fire and smoke decision support tool [20-21]. We adapt D-SHIELD and integrate with modeling tools like WRFx to make an intelligent and responsive NOS for wildfire monitoring. We demonstrate our product by tasking the CYGNSS mission [6], whose instruments are nominally always kept ON in a low data volume gathering mode (information compressed with loss) but can switch to a higher volume mode called *RawIF*, where raw observations can be retained for locations of interest and downlinked.

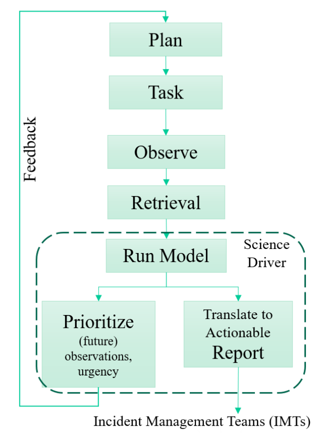

Figure 1: D-SHIELD based NOS

2. CONCEPT OF OPERATIONS

Our concept enables the simultaneous execution of missions with different data latency and urgency requirements (Figure 2). The pre-fire mission gathers high-res data at strategic locations and times at 2-6d latency while active-fire mission is for region-specific, adaptive sensing with <24h latency, 6-30h response times.

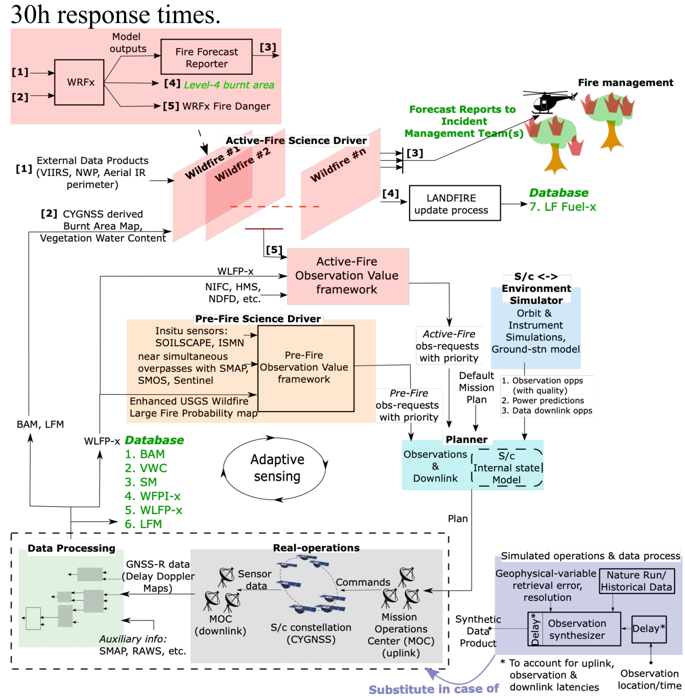

Figure 2: Concept of operations for Pre and Active Fire Missions

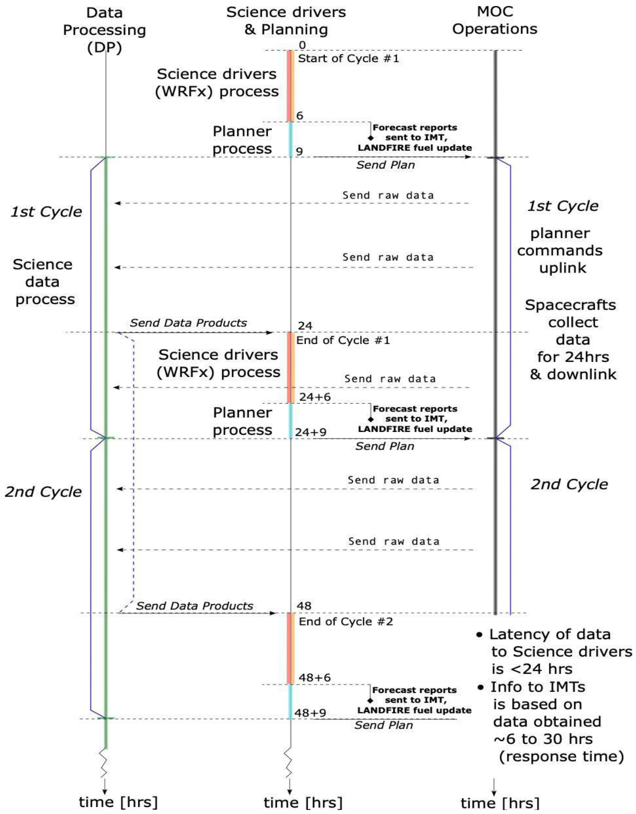

Figure 3: Timeline of Operations for Wildfire Missions

3. GNSS-R DATA INFUSION IN PRE/ ACTIVE WILDFIRE MODELS

The data pipeline (Figure 4) starts with RawIF data collected from prioritized active/ pre fire areas, followed by using it to retrieve BAM, SM and VWC. These are then processed to fire danger products (Live fuel moisture or LFM, wildfire potential index or WFPI, WFPI-based large fire probability or WLFP) and a high cadence LANDFIRE fuel layer product.

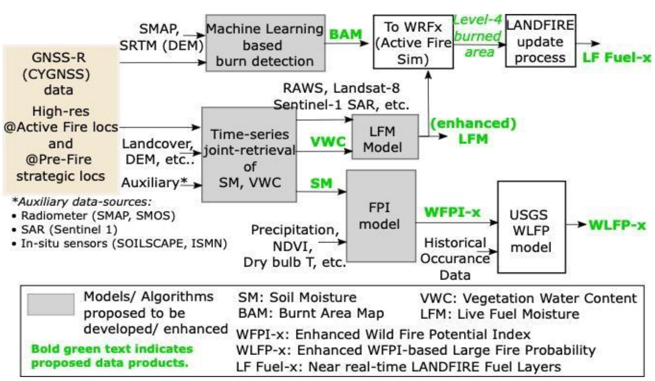

Figure 4: Data product pipeline

3.1. Burned Area Map (BAM)

BAM in the form of tuples of <time, latitude, longitude, burned/not burned, associated estimation uncertainty and area (polygon representation)> is computed over active-fire areas using GNSS-R observations from CYGNSS. This provides an indirect estimation of the fire perimeter which forms a useful input to fire-spread models. exploratory analysis depicted a reduction in reflectivity during burn periods. The CYGNSS specular point (SP) incidence angle, signal-to-noise ratio (SNR), reflectivity of SP, and spatiotemporal parameters of SP were considered as covariates. Additionally, the soil moisture, vegetation water content, surface temperature from the NASA Soil Moisture Active Passive (SMAP) mission, and elevation from the Shuttle Radar Topography Mission (SRTM) were used as ancillary data layers. Two machine learning models, random forest [15] and XGBoost [16], were trained using these feature variables to classify pixels into burned or not burned categories. The results were validated using the MODIS/Terra+Aqua Burned Area Monthly L3 Global 500 m SIN Grid [17] and MODIS Fire_cci Burned Area Pixel (version 5.1) [18] products. Figure 5 shows an example of burned area classification from the XGBoost model.

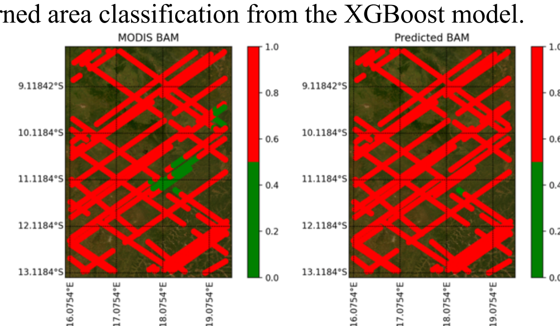

Figure 5: Burned area predicted by XGBoost model (right) with CYGNSS variables for June 1, 2019, at Angola (agricultural fires). Left plot is the MODIS BAM (truth) data. Red indicates burned; green indicates not burned.

3.2. Joint Soil Moisture (SM) and Vegetation Water Content (VWC)

The current SM retrieval algorithms from CYGNSS use VWC measured by MODIS [13,14]. We are working on a joint retrieval algorithm to retrieve SM and VWC from multiple CYGNSS observations, which is expected to yield better SM estimates along with brand new VWC data product from GNSS-R data. Observations will be selected such that they are spatially and temporally close, and joint retrievals will take advantage of other satellite and ancillary data sources (including MODIS and/or Sentinel-1 products), using both physics-based and ML-based methods.

3.3. Enhanced USGS Wildland Fire Potential Index (WFPI-x), WFPI-based Large Fire Probability (WLFP-x)

The U.S. Geological Survey (USGS) fire danger forecast model produces a 7-day fire-danger forecast for WFPI, WLFP, and fire spread probability (WFSP)[12]. The WFPI model combines measures of vegetation deadness and dryness with forecasted weather conditions from 1-7 days. We have revised the WFPI model to incorporate deviations w.r.t historical record) in SM as a modifier to the dead fuel moisture term, resulting in a WFPI-x process that incorporates SM from CYGNSS in near real-time. WLFP-x and WFSP-x are then calculated from the revised WFPI-x data (example Figure 6).

3.4. Live Fuel Moisture (LFM)

LFM is a critical input into fire spread models and fire danger products. It affects the overall fuel moisture content which in turn controls the fire rate of spread and fire intensity. The conversion between the live and dead fuel load for dynamic fuels is performed based on the LFM content. However, live fuel moisture observations are very sparse and labor intensive as they require destructive sampling of living plants, weighting the samples, over-drying them, and weighing them again. Hence, satellite products are often used in conjunction with machine learning to generate live fuel moisture maps. Our current LFM model uses all Landsat-8/9 bands, Sentinel-1 SAR backscattering, long-term weather data layers from HRRR, and multiple LANDFIRE static data layers, including topography and fuel properties, to create bi-weekly fuel moisture maps. To leverage the satellite derived VWC for LFM assessment, we will retrain the random forest LFM ML model using direct LFM observations from fuel sampling, and enhanced satellite data including the WVC. We expect that VWC can be indicative of the LFM content and therefore an important input to improve model accuracy.

3.5. High cadence LANDFIRE Fuel Layers (LF Fuel-x)

In a typical wildfire scenario, the WRF-SFIRE coupled fire atmosphere model is executed cyclically within the WRFx forecasting framework to provide twice-daily fire spread and air quality forecasts for selected fire events. At the beginning of each forecast, the fire component of the model is initialized based on the most recent airborne fire observations and satellite fire detections WRF-SFIRE uses the LANDFIRE fire behavior fuel model data to represent surface fuel characteristics. LANDFIRE fuels data are updated annually to incorporate changes from primarily landscape disturbance. We use the LANDFIRE update process with BAMs derived from CYGNSS to develop near real-time updates to the LANDFIRE fuels data for use in WRF-SFIRE model runs.

4. WILDFIRE MONITORING SCIENCE DRIVERS

The science drivers (1) produce prioritized observation requests via an ‘observation value framework’ and (2) produce actionable reports for fire management decisions.

4.1. Pre-fire science driver

The pre-fire science driver consists solely of an observation value framework. The framework considers (enhanced) USGS. fire-danger forecasts and prioritizes areas with high fire danger. This allows for enhanced data collection which can be used in active-fire forecast models in case of fire breakouts, and further refinement of the fire danger values. It also considers times and locations of near simultaneous crossovers of GNSS-R satellites with other sensing platforms (SMAP, Soilscape, Sentinel). Co-located and near coincident measurements help in better retrievals and calibrations.

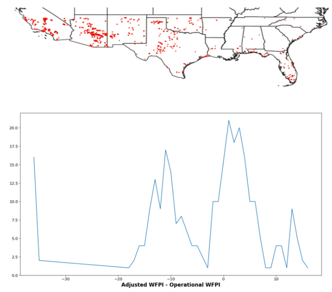

Figure 6 [Top] Map of historical wildfire events (from MTBS) in 2018-21 at CYGNSS accessible latitudes. [Bottom] Histogram of adjustments of the WLFP value across all these events

4.2. Active-fire science driver

Active fire models (WRFx which utilizes WRF-SFIRE) are executed over potentially simultaneously occurring wildfire events. The forecasted data (fire perimeters, air-quality, etc.) is transformed into actionable reports for Incident Management Teams (IMTs) responsible for managing the fire. The goal is to select and summarize the huge amounts of numerical data output from the fire forecast model into succinct reports, which are quickly comprehendible, as well as build an improved emission module within WRFx which can issue improved Air Quality (AQ) forecasts. The active fire observation value framework will be developed to prioritize observations amongst several ongoing wildfire events. This will consider information from the National Interagency Fire Center (NIFC), and the fire danger forecast from U.S.G.S. (WFPI, WLFP, WSFP). Additionally, the fuel moisture data assimilation system run within the WRFx system generates hourly dead fuel moisture maps that can inform the flight planner. In case of multiple ongoing fire events being forecasted within the WRFx system, the 48h fire spread forecasts could be also used to prioritize satellite data collection over the regions of the most active fires.

5. PLANNING SATELLITE OPERATIONS

5.1. Spacecraft orbit and access Simulations

Key pieces of orbit-related information required for optimizing satellite operations are the (1) the locations which are expected to be observed at a given (future) time and (2) contact opportunities to ground-stations to downlink data. We use an improved version of the Earth Observation Simulator (EO-Sim) to calculate these [7,8,9,10]. GNSS-R coverage calculation is unlike traditional coverage calculations, in that it requires the calculation of locations of the specular points. The spacecraft (GNSS-R and the GNSS) positions during the entire mission period, at a predefined time-step are calculated based on orbit propagation model (J2 analytical). At each time-point, specular point locations for each pair possible pair of GNSS-R & GNSS satellites are calculated, assuming a spherical Earth geometry, using the geometric formulation given in [11]. Typically, access information is required over a grid of points laid out over regions (on surface of Earth) of interest. A ‘circle of influence’ is considered about the specular point, and the grid-points within this circle are computed. If these grid-points fall within the GNSS-R antenna’s field of view, they are considered an observation opportunity at the time.

5.2. Spacecraft system Modeling

The internal data and power state of each spacecraft is modeled, per the equations below, to inform about the effect of the decisions of satellite operations. The CYGNSS system parameter values are shown in brackets.

DataStore(t+dt)=DataStore(t)+DataRateIn*dt+DownlinkRate *dt
[0 < DataStore (t) < DataStoreMax, $\forall t$]

where, DataStore: amount of data stored in onboard storage.
DataRateIn: Data generation rate during observation (96.2172 Mbps for rawIF mode; port + starboard)
DownlinkRate: Download rate to ground-station (4Mbps)
DataStoreMax: Max data accommodated onboard (5772 Mb)

Ebatt(t+dt) = Ebatt(t) + Pin *dt – Pmisc *dt - Pobs *dt– Pdwl*dt
[EbattMin < Ebatt(t) < EbattMax, $\forall t$]

where, Ebatt: energy in the battery
Pin: incoming (average) power to charge the battery from Solar panels (70W outside eclipse, and 0W when in eclipse)
Pobs: energy consumed while instrument in ON (12 W)
Pdwl: energy consumed while downlinking (15 W)
Pmisc: energy consumed by other satellite ops (26.3 W)
EbattMax: maximum battery capacity (86.4 Watt-hour)
EbattMin: minimum battery capacity, below which spacecraft goes into safe-mode (55% of max)

5.3. Satellite operations Planning and Execution

The function of the planner is to schedule the observations and data downlinks. It aims to maximize the aggregate science value for all observations, subject to resource (power/data storage capacity, solar-power generation/downlink rate) and physical (limited opportunities to observe and downlink) constraints. [4, 5] planned observations by a constellation of Synthetic Aperture Radar (SAR) satellites over a spatial domain encompassing majority of Earth's land surface, represented by a set of discrete point locations that was assigned a scientific value for the purpose of effective soil-moisture monitoring. Satellites had the ability to slew and collect rewards which varied based on the observation angle. Dynamic Constraint Processing and Mixed Integer Programming approaches were considered. For the current work, we integrated observation and downlink planning using the Propel-MCTS planning approach. A binary decision variable is defined for every time point when a satellite can (a) collect data or not, or (b) downlink data or not. MCTS is adapted as the search engine to explore the huge search space (28,234 binary decision variables => 2^28,234 nodes) [13]. A new version of Propel [2, 3] which incorporates MCTS is used to embed non-deterministic choice points (assignment statements) anywhere in Python. To speed up the planner execution, MCTS Tree parallelization is used. The satellite operations plan is sent to the Mission Operations Center (MOC), where it is verified, translated to lower-level operation commands and uplinked to the respective satellites in the distributed satellite system. Observational data is downlinked from the satellites to the commanded ground-stations. The raw data is processed to higher level science data products and are fed back to the respective science models (USGS WFPI model, WRFx), and may be databased for public access.

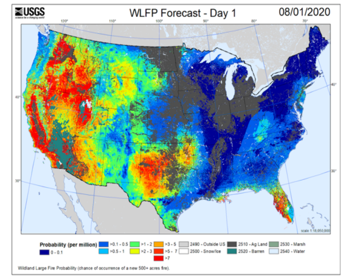

Figure 7: USGS WLFP forecast (day 1) of 1 Aug 2020.

5.4. Simulated Example

We ran the planner on a Pre-fire scenario with a system of 4 satellites (based on CYGNSS), generating coordinated plans for all satellites for a 12-hour period on 1 Aug 2020. The science driver is the WFPI-based Large Fire Probability (WLFP) (fire-danger) forecast data (Figure 7) produced by the U.S. Geological Society (USGS), The planner maximizes the aggregate WLFP for all observed targets. The fine 1km grid is upscaled by a factor of 1/10 (upper limited by the size of the sensor footprint), to yield 47k grid points to reduce the spatial scale of the problem. Locations with higher fire danger value are prioritized to obtain pre-fire data products. GNSS-R coverage calculations from reflections of GPS, Galileo GNSS satellite systems is considered. A circle of influence of 25km and the (upscaled) USGS fire-danger grid-points within this circle are calculated. Three Prioranet ground stations are considered for downlink in Hawaii, Chile, and Western Australia. A centralized, ground-based planner generates coordinated observation and downlink plans for all satellites in the system which maximizes the sum of values of all images within a plan. Half an image's value is collected when it is observed, and another half when downlinked (pro-rated by % downlinked). Coordination avoids duplicate observations of targets. Figure 8 shows the objective score versus #rollouts with ~20% improvement observed compared to a baseline case with 1 rollout. The improvement in the objective score comes at the cost of planning time.

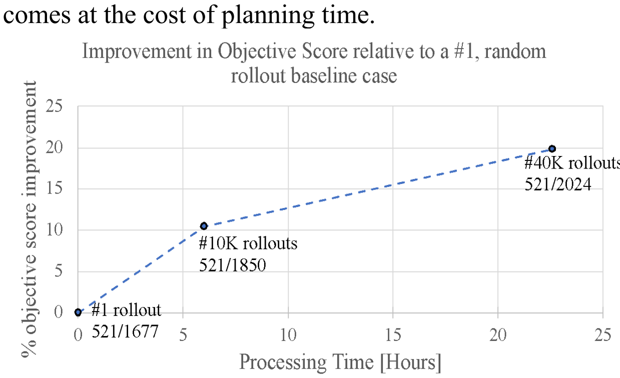

Figure 8: Objective score versus planner execution time. ~20% improvement is seen with greater # rollouts, and hence reinforcement learning.

D-SHIELD for Wildfires is currently at TRL3.

8. REFERENCES

[1] S. Nag, M. Moghaddam, D. Selva, J. Frank, V. Ravindra, R. Levinson, A. Azemati, A. Aguilar, A. Li, R. Akbar, "D-SHIELD: Distributed Spacecraft with Heuristic Intelligence to Enable Logistical Decisions", IEEE International Geoscience and Remote Sensing Symposium, Hawaii USA, July 2020

[2] Levinson R. 2005. Unified Planning and Execution for Autonomous Software Repair, ICAPS 2005, Workshop on Plan Execution.

[3] Levinson, R., 2020. Integrated Planning, Execution and Goal Reasoning for Python. ICAPS 2020, workshop on Integrated Execution (IntEx).

[4] Levinson, R., Niemoeller, S., Nag, S., Ravindra, V. (2022, June). Planning Satellite Swarm Measurements for Earth Science Models: Comparing Constraint Processing and MILP Methods. In Proceedings of the International Conference on Automated Planning and Scheduling (Vol. 32, pp. 471-479).

[5] Levinson, R., Nag, S., and Ravindra, V. 2021. Agile Satellite Planning for Multi-payload Observations for Earth Science, Proceedings of the International Workshop on Planning and Scheduling for Space (IWPSS). 2021.

[6] Ruf, C. S., Chew, C., Lang, T., Morris, M. G., Nave, K., Ridley, A., Balasubramaniam, R. (2018). A new paradigm in earth environmental monitoring with the CYGNSS small satellite constellation. Scientific reports, 8(1), 8782.

[7] Ravindra, V., Ketzner, R., Nag, S. (2021, July). Earth Observation Simulator (EO-Sim): An Open-Source Software for Observation Systems Design. In 2021 IEEE International Geoscience and Remote Sensing Symposium IGARSS (pp. 7682-7685). IEEE.

[8] Ketzner, Ryan, Vinay Ravindra, and Michael Bramble. "A robust, fast, and accurate algorithm for point in spherical polygon classification with applications in geoscience and remote sensing." Computers & Geosciences 167 (2022): 105185.

[9] Cell-Based Preprocessing Algorithm for Fast Satellite Coverage Calculation, accepted at IEEE Aero 2024.

[10] Ravindra, V., & Nag, S. (2020, March). Instrument data metrics evaluator for tradespace analysis of earth observing constellations. In 2020 IEEE Aerospace Conference (pp. 1-20). IEEE.

[11] David Eberly (2022, May). Alhazen’s Problem: Reflection Point on a Sphere. Geometric Tools, Redmond WA. https://www.geometrictools.com/Documentation/SphereReflections.pdf

[12] U.S. Geological Survey. (n.d.). Fire Danger Forecast. Retrieved from https://www.usgs.gov/fire-danger-forecast

[13] C. Chew and E. Small, “Description of the UCAR/CU Soil Moisture Product,” Remote Sens (Basel), vol. 12, no. 10, p. 1558, May 2020, doi: 10.3390/rs12101558.

[14] P. T. Setti and S. Tabibi, "Incidence Angle Normalization of Spaceborne GNSS-R Surface Reflectivity for Soil Moisture Retrieval," IGARSS 2023 - 2023 IEEE International Geoscience and Remote Sensing Symposium, Pasadena, CA, USA, 2023, pp. 510-513, doi: 10.1109/IGARSS52108.2023.10282074.

[15] L. Breiman, “Random forests,” Machine learning, vol. 45, pp. 5–32, 2001.

[16] T. Chen and C. Guestrin, “Xgboost: A scalable tree boosting system,” in Proceedings of the 22nd ACM sigkdd International Conference on Knowledge Discovery and Data Mining, pp. 785–794, 2016.

[17] L. Giglio, C. Justice, L. Boschetti, and D. Roy, “Modis/terra+ aqua burned area monthly l3 global 500m sin grid v061 [data set],” NASA EOSDIS Land Processes DAAC: Washington, DC, USA, 2021.

[18] M. Pettinari, J. Lizundia-Loiola, and E. Chuvieco, “ESA CCI ECV fire disturbance: D4. 2 product user guide-MODIS, version 1.1,” 2021.

[19] Rémi Coulom (2006). "Efficient Selectivity and Backup Operators in Monte-Carlo Tree Search". Computers and Games, 5th International Conference, CG 2006, Turin, Italy, 2006.

[20] Jan Mandel, Martin Vejmelka, Adam K. Kochanski, Angel Farguell, James D. Haley, Derek V. Mallia, and Kyle Hilburn. An interactive data-driven HPC system for forecasting weather, wildland fire, and smoke. In 2019 IEEE/ACM HPC for Urgent Decision Making (UrgentHPC), Denver, CO, USA, pages 35–44. IEEE, 2019.

[21] Mandel, J., Beezley, J. D. and Kochanski, A. K. (2011), Coupled atmosphere-wildland fire modeling with WRF 3.3 and SFIRE 2011. Geosci. Model Dev., 4, 591—610.

[22] S. Nag, A. S. Li, V. Ravindra, M. Sanchez Net, K.M. Cheung, R. Lammers, B. Bledsoe, Autonomous Scheduling of Agile Spacecraft Constellations with Delay Tolerant Networking for Reactive Imaging, International Conference on Automated Planning and Scheduling SPARK Workshop, Berkeley CA, July 2019

[23] R. Lammers, A.S. Li, V. Ravindra, S. Nag, Prediction Models for Urban Flood Evolution for Satellite Remote Sensing, Journal of Hydrology 603 (2021), pp 127175

[24] V. Ravindra, S. Nag and A. Li, Ensemble-Guided Tropical Cyclone Track Forecasting for Optimal Satellite Remote Sensing, in IEEE Transactions on Geoscience and Remote Sensing, vol. 59, no. 5, pp. 3607-3622, May 2021